

Wilson Loops, Geometric Transitions and Bubbling Calabi-Yau's

Jaume Gomis¹ and Takuya Okuda²

Perimeter Institute for Theoretical Physics
Waterloo, Ontario N2L 2Y5, Canada¹

and

Kavli Institute for Theoretical Physics
University of California, Santa Barbara
CA 93106, USA²

Abstract

Motivated by recent developments in the AdS/CFT correspondence, we provide several alternative bulk descriptions of an arbitrary Wilson loop operator in Chern-Simons theory. Wilson loop operators in Chern-Simons theory can be given a description in terms of a configuration of branes or alternatively anti-branes in the resolved conifold geometry. The representation of the Wilson loop is encoded in the holonomy of the gauge field living on the dual brane configuration. By letting the branes undergo a new type of geometric transition, we argue that each Wilson loop operator can also be described by a bubbling Calabi-Yau geometry, whose topology encodes the representation of the Wilson loop. These Calabi-Yau manifolds provide a novel representation of knot invariants. For the unknot we confirm these identifications to all orders in the genus expansion.

¹jgomis at perimeterinstitute.ca

²takuya at kitp.ucsb.edu

Contents

1	Introduction, summary and conclusion	1
2	Wilson loops as branes in the deformed conifold	6
2.1	Wilson loops as D-branes	8
2.2	Wilson loops as anti-branes	10
3	Wilson loops as branes in the resolved conifold	11
4	Wilson loops as bubbling Calabi-Yau's	13
A	Wilson loops as world-sheet instantons	16
B	Wilson loops as crystals	18
C	Target space theory of open topological strings	20

1 Introduction, summary and conclusion

The study of quantum gravity using a holographic formulation requires understanding how the bulk gravitational physics is described by the boundary gauge theory. Given the ubiquitous nature of Wilson loop operators in gauge theory, it is of interest to understand how Wilson loop operators in a gauge theory participating in the holographic formulation of a bulk theory are encoded in the corresponding bulk description. Since gauge theories can be formulated using Wilson loops as the basic variables, an improved understanding of holography may arise from identifying these variables in the bulk theory.

This program has recently been completed in [1] for all half-BPS Wilson loop operators in $\mathcal{N} = 4$ SYM (for previous work see [2, 3]). This extends the bulk description of a Wilson loop in the fundamental representation in terms of a string world-sheet [4, 5] to all other representations. It was found that for each Wilson loop, there is a bulk description either in terms of a configuration of D5-branes or alternatively in terms of a configuration of D3-branes in $\text{AdS}_5 \times S^5$ (see [1] for details). The equations determining the supergravity background produced by these D-branes were found in [3, 6] (see also [7] for the closely related equations for half-BPS domain wall operators), generalizing the supergravity solutions of LLM [8] dual to half-BPS local operators to half-BPS Wilson loop operators. All these asymptotically $\text{AdS}_5 \times S^5$ solutions encode in their nontrivial topology the information about the dual operator. For other work see e.g. [9, 10, 11, 12, 13, 14, 15].

A very interesting and calculable example of a holographic correspondence is the one

found by Gopakumar and Vafa [16] in topological string theory³. The duality states that the A-model topological string theory on the deformed conifold T^*S^3 in the presence of N D-branes wrapping S^3 is dual to the A-model topological string theory on the resolved conifold geometry, with the complexified Kähler modulus given by $t = g_s N$, where g_s is the string coupling constant on both sides of the correspondence. As shown by Witten [19], the physics on the deformed conifold is described by $U(N)$ Chern-Simons theory on S^3 .

The goal of this paper is to give the bulk description of Wilson loop operators in Chern-Simons theory⁴. As we shall see, a picture closely related to the one for $\mathcal{N} = 4$ SYM emerges, with the added benefit that we have control over all quantum corrections for the case of Chern-Simons theory. We find that Wilson loops in Chern-Simons can be described either in terms of a configuration of D-branes or a configuration of anti-branes in the resolved conifold geometry. Moreover, by letting the branes undergo a geometric transition, we find that Wilson loops can be described in terms of bubbling Calabi-Yau geometries, with rich topology.

We first identify the holographic description of Wilson loop operators in Chern-Simons theory on S^3 – labeled by a knot in S^3 and a representation of $U(N)$ – in terms of branes in the resolved conifold geometry. Just like in [1], we find that there are two different brane configurations corresponding to each Wilson loop operator.

The information about the knot $\alpha \subset S^3$ is encoded in the choice of a Lagrangian submanifold L in the resolved conifold geometry, as explained by Ooguri and Vafa in [20] (see also e.g. [21, 22, 23]). L ends on the knot α on the S^3 at asymptotic infinity of the resolved conifold geometry, where the holographic dual Chern-Simons theory lives⁵.

We show that the information about the representation R of the Wilson loop operator – given by a Young tableau (see Figure 1) – is encoded in the eigenvalues⁶ of the holonomy matrix obtained by integrating the gauge connection on the branes wrapping L – denoted by \mathcal{A} – around the non-contractible β -cycle⁷ of the Lagrangian submanifold L .

We show that a Wilson loop labeled by a knot α and a representation R given by Figure 1 is described either by a configuration of M D-branes $(L_{x_1}, L_{x_2}, \dots, L_{x_M})$ or by a configuration of P anti-branes $(\overline{L}_{y_1}, \overline{L}_{y_2}, \dots, \overline{L}_{y_P})$, where $L_{x_i}/\overline{L}_{y_i}$ denotes a D-brane/anti-

³See [17] for an overview of results and the book [18] by Mariño for a comprehensive introduction.

⁴As suggested in [16], the Wilson loops can be described by string world-sheets in the resolved conifold. We elaborate on this description in Appendix A.

⁵Taubes [24] proposed a procedure to construct the Lagrangian submanifolds corresponding to the knots that are invariant under the antipodal map of S^3 . The construction of the Lagrangians corresponding to arbitrary knots was achieved by Koshkin [25].

⁶Geometrically, these eigenvalues correspond to the positions of the branes up to Hamiltonian deformations (see Appendix C).

⁷ L has the topology of a solid torus with a boundary at infinity given by a T^2 with canonical α and β one cycles. The β cycle is non-contractible in L while α may or may not be contractible.

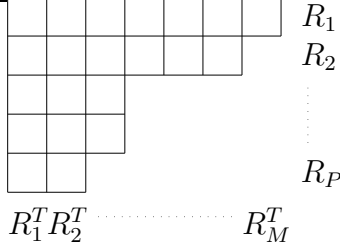


Figure 1: A Young tableau with $P \leq N$ rows and M columns labeling a representation of $U(N)$. R_i is the number of boxes in the i -th row and satisfies $R_i \geq R_{i+1}$. R^T is the tableau conjugate to R , obtained by exchanging rows with columns.

brane with world-volume L and with a non-trivial holonomy, shifted by the integral of the Kähler form \mathcal{J} ,

$$x_i \equiv \oint_{\beta=\partial D} \mathcal{A}_i + \int_D \mathcal{J} = g_s \left(R_i^T - i + M + \frac{1}{2} \right), \quad i = 1, \dots, M, \quad (1.1)$$

$$y_i \equiv \oint_{\beta=\partial D} \mathcal{A}_i + \int_D \mathcal{J} = g_s \left(R_i - i + P + \frac{1}{2} \right), \quad i = 1, \dots, P, \quad (1.2)$$

respectively⁸.

For the case of the simplest knot – the unknot – we explicitly check this identification. We show that this Wilson loop operator in a representation given by Figure 1 corresponds to the configuration of M D-branes $(L_{x_1}, L_{x_2}, \dots, L_{x_M})$

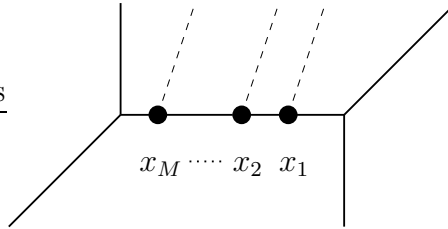


Figure 2: Brane configuration in resolved conifold describing Wilson loop in a representation given by Figure 1.

where L_{x_i} denotes a D-brane wrapping a Lagrangian submanifold L sitting at the position $x_i = g_s(R_i^T - i + M + 1/2)$ on the inner edge of the toric diagram of the resolved conifold. In particular, a single D-brane on the inner edge corresponds to a Wilson loop in the antisymmetric representation. Since the effective size of the inner edge of the resolved

⁸ \mathcal{J} is integrated over a disk D . D is a relative cycle in the resolved conifold and has $\beta \subset L$ as its boundary.

conifold is $t_{eff} = g_s(N + 1)$, we recover (from $x_1 \leq t_{eff}$) the group theory bound $R_1^T \leq N$ for the number of boxes in a column from the compactness of the \mathbf{P}^1 of the resolved conifold.

The same Wilson loop operator can also be described by a configuration of P anti-branes $(\overline{L}_{y_1}, \overline{L}_{y_2}, \dots, \overline{L}_{y_P})$

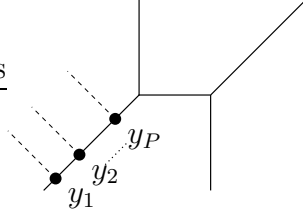


Figure 3: Brane configuration in resolved conifold describing Wilson loop in a representation given by Figure 1.

where \overline{L}_{y_i} denotes an anti-brane wrapping a Lagrangian submanifold L sitting at the position $y_i = g_s(R_i - i + P + 1/2)$ on an outer edge of the toric diagram. In particular, a single D-brane on the outer edge corresponds to a Wilson loop in the symmetric representation. Since the outer edge is non-compact, R_1 can be an arbitrarily large integer, as expected from group theory. The bound on the number of anti-branes $P \leq N$ can also be understood geometrically. Once we put P anti-branes in the resolved conifold, the effective size of the space is $t_{eff} = g_s(N - P)$, thus recovering the group theory bound $P \leq N$.

These results are obtained by computing the A-model topological string partition function in the presence of these branes and showing that it agrees with the Chern-Simon results of Witten [19]. In the crystal melting description [26, 27] of these amplitudes, the Young tableau of the dual Wilson loop has a nice geometrical realization in the crystal. The corners produced in the crystal by the insertion of branes [28, 27] has exactly the shape of the corresponding Young tableau!

We also find a purely geometric description of the unknot Wilson loop operators in terms of Calabi-Yau geometries that are asymptotic to the resolved conifold. We show that the backreaction of the brane configurations in Figures 2 and 3 can be taken into account exactly, giving rise to a Calabi-Yau geometry without D-branes! The two different D-brane configurations in Figures 2 and 3 yield the same Calabi-Yau geometry, and the information about the representation R of the Wilson loop is now encoded in the topology of the corresponding Calabi-Yau. Physically, the appearance of this rich class of Calabi-Yau geometries can be understood as arising from a new class of geometric transitions, where non-compact Lagrangian D-branes/anti-branes are replaced by non-trivial topologies supporting the “flux” produced by the branes. The computation

of the A-model topological string amplitude on these “bubbling” Calabi-Yau geometries, obtained by letting the branes undergo a geometric transition, exactly reproduces the result for the expectation value of the corresponding Wilson loop obtained by Witten [19]. Therefore, these bubbling Calabi-Yau geometries provide a novel representation of knot invariants of Chern-Simons theory.

The topology of the Calabi-Yau geometry corresponding to a Wilson loop is best understood by giving the following parametrization of a Young tableau⁹

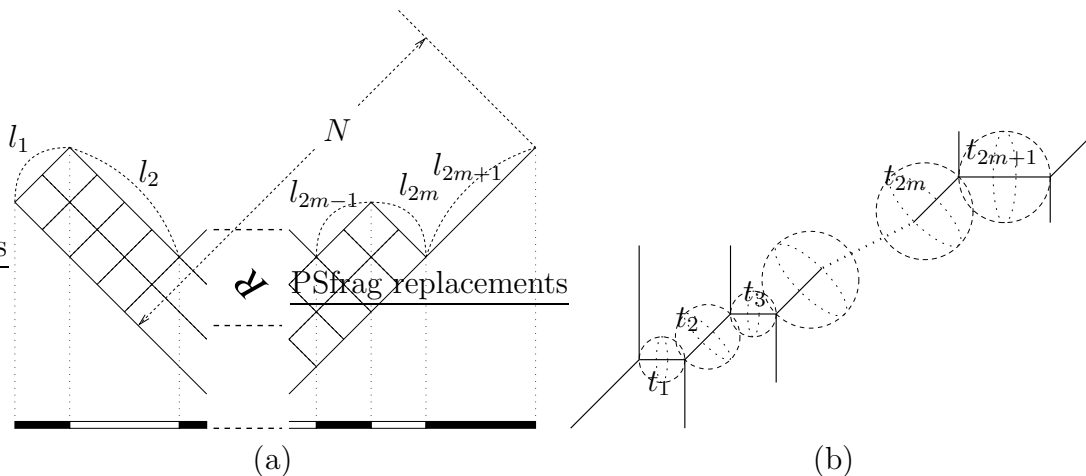


Figure 4: The correspondence of the Wilson loop in representation R and the bubbling geometry. In (a) the Young tableau R , shown rotated, is specified by the lengths l_i of all the edges. l_{2m+1} is N minus the number of rows. Equivalently, l_i are the lengths of black and white regions in the Maya diagram. The Wilson loop in representation R (a) is equivalent to the toric Calabi-Yau manifold given by the web diagram (b). There are a total of $2m + 1$ bubbles of \mathbf{P}^1 in the geometry. The sizes of the \mathbf{P}^1 's are given by $t_i = g_s l_i$, $i = 1, \dots, 2m + 1$.

The Calabi-Yau geometry dual to a Wilson loop labeled by a Young tableau given in Figure 4(a) is given by the toric web diagram shown in Figure 4(b). The corresponding Calabi-Yau geometry has $2m + 1$ nontrivial \mathbf{P}^1 's. The associated complexified Kähler moduli are given by $t_i = g_s l_i$ for $i = 1, \dots, 2m + 1$, where l_i are the integers in Figure 4(a) parametrizing the Young tableau. Similarity between bubbling AdS geometries and toric geometries was noted in [8].

Although the explicit quantitative checks we make are all based on the unknot, our physical arguments apply to arbitrary knots and links. Indeed it is possible to write the closed Gopakumar-Vafa (GV) invariants [16] associated to the bubbling Calabi-Yau corresponding to an arbitrary knot in terms of the open GV invariants [20, 22] associated

⁹Informally, l_{odd} is the number of rows in the tableau with the same number of boxes while l_{even} is the number of columns in the tableau with the same number of boxes.

to the Lagrangian branes giving rise to the bubbling Calabi-Yau after geometric transition. We plan to report on this relation and on more general geometric transitions in the forthcoming paper [29].

The extent of the analogy between AdS/CFT and the GV duality is striking. We hope that the very explicit realization of the holographic correspondence found in this paper – including all quantum corrections – provides us with hints for deeper understanding of the AdS/CFT correspondence and holography in further detail.

The plan of the rest of the paper is as follows. In section 2 we integrate out the degrees of freedom introduced by a configuration of non-compact branes intersecting S^3 along a knot α and show that the net effect is to insert a Wilson loop operator for $U(N)$ Chern-Simons theory on S^3 . In section 3 we identify the brane configurations in the resolved conifold dual to a Wilson loop operator. The identification is explicitly checked for the case of the unknot. In section 4 we show that the Wilson loop operators can be related to the closed string partition function of bubbling Calabi-Yau's, which are interpreted as arising via a geometric transition of the brane configuration in section 3. Appendix A revisits the description of Wilson loops in terms of string world-sheets. Appendix B reviews the melting crystal models found in [27]. The explicit computations for the unknot, which support our proposal in this paper, are performed using the crystal models. Appendix C explains relevant details of the target space theory of open topological strings.

2 Wilson loops as branes in the deformed conifold

In this section we find a brane configuration in T^*S^3 whose effective description is given by a Wilson loop operator of Chern-Simons theory on S^3 . The basic idea is to add extra non-compact branes beyond the N D-branes wrapping the S^3 that support the $U(N)$ Chern-Simons theory participating in the large N duality. We show that integrating out the degrees of freedom introduced by the extra branes has the effect of inserting into the $U(N)$ Chern-Simons path integral on S^3 a Wilson loop operator in a particular representation R of $U(N)$ determined by data of the brane configuration. Having identified the brane configuration in T^*S^3 corresponding to a Wilson loop, in the next section we find the holographic description of Wilson loops in terms of branes in the resolved conifold.

A Wilson loop operator of Chern-Simon theory on S^3 is labeled by a representation R of $U(N)$ and by an embedded oriented circle α – also known as a knot – in S^3 . It is given by

$$W_R(\alpha) = \text{Tr}_R P \exp \oint_{\alpha} A, \quad (2.3)$$

where P is the path ordering operator.

A microscopic description of a Wilson loop operator can be given by adding new degrees of freedom localized on the knot on which the operator is supported. In the string theory realization, the new localized degrees of freedom arise microscopically by quantizing open strings between the D-branes wrapping S^3 and new branes intersecting the S^3 along the knot α .

As shown by [20], a Lagrangian submanifold L in T^*S^3 can be found such that it intersects S^3 along an arbitrary knot α . Given a knot α in S^3 parametrized by $q^i(s)$, where q^i are coordinates on S^3 , then L is determined by the following non-compact Lagrangian submanifold¹⁰

$$L = \{(q^i, p_i) \mid \sum_i^3 p_i \frac{dq^i}{ds} = 0\}, \quad (2.4)$$

where p_i are coordinates in the fiber of T^*S^3 . The topology of L is $\mathbb{R}^2 \times S^1$ or more precisely that of a solid torus. The brane is non-compact and has a boundary at asymptotic infinity. The boundary is a T^2 with canonical α and β one cycles. In L , the α -cycle of the T^2 is non-contractible while the β -cycle of the T^2 is contractible¹¹.

Therefore, we want to consider the gauge theory living on the brane configuration in T^*S^3 given by N D-branes wrapping S^3 intersecting M branes wrapping L . The action is given by [20]

$$S = S_{CS}(A) + S_{CS}(\mathcal{A}) + \oint_{\alpha} \chi^\dagger (d + A + \mathcal{A}) \chi, \quad (2.5)$$

where

$$S_{CS}(A) = \frac{1}{g_s} \int_X \text{Tr} \left(A \wedge dA + \frac{2}{3} A \wedge A \wedge A \right), \quad (2.6)$$

and A, \mathcal{A} are the connections on $X = S^3$ and $X = L$ respectively. χ are bifundamental fields localized along the knot α arising from the quantization of open strings with one end on S^3 and the other one on L . Depending on whether we wrap a D-brane or an anti-brane¹² on L , χ is either a fermionic or bosonic field.

¹⁰We recall that the Kähler form of T^*S^3 is given by $\omega = \sum_{i=1}^3 dp_i \wedge dq^i$.

¹¹As we will see in the next section, the roles of α and β are reversed in the corresponding Lagrangian submanifold L in the resolved conifold; β being non-contractible in the corresponding L .

¹²In topological string theory an anti-brane is exactly the same [30, 31] as a ghost brane, obtained by reversing the sign of the D-brane boundary state. That's why the statistics of the open string fields is reversed when open strings are stretched between a D-brane and an anti-brane as compared to when they are stretched between two D-branes.

2.1 Wilson loops as D-branes

If D-branes wrap L then χ are fermions. Integrating out χ is straightforward, it inserts the so called Ooguri-Vafa operator [20]¹³

$$\sum_Q \text{Tr}_{Q^T} P \exp \oint_\alpha A \cdot \text{Tr}_Q P \exp \oint_\alpha \mathcal{A}, \quad (2.7)$$

where Q^T is the Young tableau conjugate to Q . We now want to integrate \mathcal{A} out¹⁴

$$e^{iS_{CS}(A)} \sum_Q \text{Tr}_{Q^T} P \exp \oint_\alpha A \cdot \int [D\mathcal{A}] e^{iS_{CS}(A)} \text{Tr}_Q P \exp \oint_\alpha \mathcal{A} \quad (2.8)$$

In order to proceed we now briefly recall some well known facts about Chern-Simons theory. In the present case, Chern-Simons is defined on a solid torus with a boundary at infinity given by a T^2 . The path integral is a wave function $\langle \psi |$ for Chern-Simons theory on a T^2 and depends on the boundary condition imposed at infinity.

The path integral in (2.8) has the insertion of $\text{Tr}_Q P \exp \oint_\alpha \mathcal{A}$, that is a Wilson loop along the non-contractible cycle α of T^2 . This creates a state of Chern-Simons theory on T^2 labeled by $|Q\rangle$. Therefore (2.8) yields

$$e^{iS_{CS}(A)} \sum_Q \text{Tr}_{Q^T} P \exp \oint_\alpha A \cdot \langle \psi | Q \rangle. \quad (2.9)$$

The holonomies around the α and β cycles of T^2 are canonically conjugate [32]. The path integral is defined by specifying the holonomy at infinity either around the α or β cycle. Roughly speaking, the holonomy around α plays the role of the position operator while the holonomy around the β cycle plays the role of momentum. In the context of Chern-Simons theory, momentum can be identified with the highest weight vector of a representation R , shifted by the Weyl vector.

Since our aim is to find the Wilson loop in a particular representation R (2.3), we choose the boundary condition $\langle \psi | = \langle R^T |$. This means that we choose a boundary condition at infinity with non-trivial holonomy around the contractible cycle β in L . Since the states labeled by representations form an orthonormal basis, this picks out the $Q = R^T$ term in (2.9). In other words, imposing the boundary condition $\langle \psi | = \langle R^T |$ is equivalent to focusing on the $Q = R^T$ term in (2.9).

We now give the physical interpretation of this boundary condition. In a nutshell, the holonomy around the contractible cycle β measures fundamental string charge.

¹³ The path integral over χ reduces to that of free fermions. This formula can then be derived by noting that $\prod_{i=1}^N \prod_{I=1}^M (1 + x_i y_I) = \sum_Q \text{Tr}_{Q^T} X \text{Tr}_Q Y$, where $X = \text{diag}(x_i)$, $Y = \text{diag}(y_I)$.

¹⁴In this analysis we omit the path integral over A , which is to be done at the end. In [20] the path integral over A was performed while the integral over \mathcal{A} wasn't.

Open String Endpoints as Anyons

To understand the physical meaning of the boundary condition, let us consider the effect of the Wilson loop $\text{Tr}_R \exp \oint \mathcal{A}$ on the non-compact branes.

Consider first the case when $M = 1$, i.e. for a single brane on L . The action of the brane in the presence of the Wilson loop (swept by an open string end point) is given by

$$S = S_{CS}(\mathcal{A}) + k \oint_{\alpha} \mathcal{A}. \quad (2.10)$$

Therefore, the corresponding equations of motion are given by

$$F_{z\bar{z}} = g_s k \delta^2(z), \quad (2.11)$$

where z is the complex coordinate parameterizing the \mathbb{R}^2 in L . Physically, the endpoint of an open string behaves like an anyon when viewed from the brane world-volume.

By integrating (2.11) we conclude that having k fundamental strings ending on L introduces a non-trivial holonomy around the contractible cycle β of the T^2 in L . The holonomy is given by

$$\oint_{\beta} \mathcal{A} = g_s k. \quad (2.12)$$

In the general case of M arbitrary, the treatment of the non-Abelian equations of motion is more subtle, as noted originally by Witten [33]. Fortunately, we can borrow results from [32], where the insertion of the Wilson loop in the representation R^T was found to induce the holonomy

$$\oint_{\beta} \mathcal{A}_i = g_s \left(R_i^T - i + \frac{1}{2}M + \frac{1}{2} \right), \quad i = 1, 2, \dots, M. \quad (2.13)$$

Therefore, the boundary condition $\langle \psi | = \langle R^T |$ is tantamount to introducing the holonomy given by (2.13) at infinity. We denote by $(L_{R_1^T}, \dots, L_{R_M^T})$ the configuration of branes with this holonomy (2.13).

When we go through the transition to the resolved conifold, we will see that there is a shift by $\frac{1}{2}g_s M$ in the effective holonomy, coming from the backreaction of the geometry on the branes. In Appendix C we show that the gauge invariant quantity is given by the holonomy shifted by the integral of the Kähler form over a disk ending on β , thus giving rise to the shift by¹⁵ $\frac{1}{2}g_s M$ in the resolved conifold.

¹⁵The shift of the Kähler modulus due to the insertion of branes is well known [34, 28, 27] and it is given by $g_s M$. Therefore, when the Kähler modulus is integrated over a disk bounding β – as opposed to over \mathbf{P}^1 – we get a shift by $\frac{1}{2}g_s M$.

Therefore, the D-brane configuration $(L_{R_1^T}, \dots, L_{R_M^T})$ we have considered in T^*S^3 inserts a Wilson loop operator along the knot α

$$e^{iS_{CS}(A)} \cdot \text{Tr}_R P \exp \oint_{\alpha} A. \quad (2.14)$$

Summarizing, we have derived the identification

$$(L_{R_1^T}, \dots, L_{R_M^T}) \leftrightarrow \text{Tr}_R P \exp \oint_{\alpha} A. \quad (2.15)$$

2.2 Wilson loops as anti-branes

In topological string theory an anti-brane has the interpretation as a ghost brane [30, 31], whose boundary state is minus that of a brane. This sign changes the statistics of the open string fields between branes and anti-branes. This is why the χ fields in the brane configuration we have described in T^*S^3 are bosonic when anti-branes wrap the Lagrangian submanifold L .

When χ are quantized as bosonic fields, integrating them out yields¹⁶

$$\sum_Q \text{Tr}_Q P \exp \oint_{\alpha} A \cdot \text{Tr}_Q P \exp \oint_{\alpha} \mathcal{A}. \quad (2.16)$$

We can now easily calculate the path integral over \mathcal{A} following our previous discussion for D-branes. If we denote by $(\bar{L}_{R_1}, \dots, \bar{L}_{R_P})$ a configuration of P anti-branes with holonomy¹⁷

$$\oint_{\beta} \mathcal{A}_i = g_s \left(R_i - i + \frac{1}{2}P + \frac{1}{2} \right), \quad i = 1, 2, \dots, P, \quad (2.17)$$

corresponding to the boundary condition $\langle \psi | = \langle R |$, we are left with the insertion of a Wilson loop operator along the knot α given by

$$e^{iS_{CS}(A)} \cdot \text{Tr}_R P \exp \oint_{\alpha} A. \quad (2.18)$$

Therefore we arrive at the identification

$$(\bar{L}_{R_1}, \dots, \bar{L}_{R_P}) \leftrightarrow \text{Tr}_R P \exp \oint_{\alpha} A. \quad (2.19)$$

We now study the bulk description of Wilson loops in Chern-Simons theory in terms of branes in the resolved conifold geometry.

¹⁶ Now the path integral over χ reduces to that of free bosons. The final answer is obtained by noting that $\prod_{i=1}^N \prod_{I=1}^M \frac{1}{1-x_i y_I} = \sum_Q \text{Tr}_Q X \text{Tr}_Q Y$.

¹⁷ As before, there will be a shift by $\frac{1}{2}g_s P$ in the resolved conifold.

3 Wilson loops as branes in the resolved conifold

In the previous section we have shown that a Wilson loop operator on any knot α and for any representation R can be obtained by integrating out the physics of a D-brane configuration $(L_{R_1^T}, \dots, L_{R_M^T})$ or anti-brane configuration $(\bar{L}_{R_1}, \dots, \bar{L}_{R_P})$.

To obtain the resolved conifold description of a Wilson loop we follow the brane configuration through the conifold singularity. It is possible to construct a Lagrangian submanifold L explicitly for every knot α in S^3 [24, 25]. Physically, this Lagrangian submanifold in the resolved conifold is the dual description of the Lagrangian submanifold (2.4) in T^*S^3 described in the previous section. Topologically L is also $R^2 \times S^1$ and has an asymptotic boundary given by a T^2 .

The Lagrangian submanifolds constructed by Taubes have the property that they end on a knot α in the S^3 at infinity. From the point of view of holography, this is precisely as expected. The dual $U(N)$ Chern-Simons theory lives on the S^3 at asymptotic infinity in the resolved conifold. Given that we are looking for the resolved conifold description of Wilson loops, it is expected that the bulk description is given by a bulk object which ends on a knot, thus introducing the appropriate source for a Wilson loop operator.

A crucial role in the derivation in the previous section is played by the holonomies around the contractible cycle of the T^2 in L

$$\oint_{\beta} \mathcal{A}_i. \tag{3.20}$$

This data has a nice geometrical interpretation in the resolved conifold. As one follows the branes through the conifold singularity, the contractible cycle β of the Lagrangian L in T^*S^3 grows to become a non-contractible cycle β of the T^2 on the corresponding Lagrangian L of the resolved conifold.

As explained in more detail in Appendix C, the holonomy of the complex gauge field \mathcal{A} has the interpretation as the modulus¹⁸ of the brane. More precisely, in addition to the holonomy of the gauge field, the gauge invariant modulus has a contribution from the Kähler form \mathcal{J} integrated over a disk ending on β . This contributes $\frac{1}{2}g_s M$ to the modulus since $\int_D \mathcal{J} = \frac{1}{2}g_s M$ (see footnote 15).

Therefore, the Wilson loop operator described by the brane configuration $(L_{R_1^T}, \dots, L_{R_M^T})$ in the deformed conifold has a bulk interpretation in terms of M Lagrangian D-branes $(L_{x_1}, \dots, L_{x_M})$ in the resolved conifold. Moreover, the modulus x_i of the i -th brane in the resolved conifold is determined by the holonomy data (2.13)

$$x_i = \oint_{\partial D=\beta} \mathcal{A} + \int_D \mathcal{J} = g_s \left(R_i^T - i + M + \frac{1}{2} \right) \quad i = 1, \dots, M \tag{3.21}$$

¹⁸In the toric diagram, the modulus is the position of the brane.

Similarly, the brane configuration $(\bar{L}_{R_1}, \dots, \bar{L}_{R_P})$ in the deformed conifold has a bulk interpretation in terms of P Lagrangian anti-branes $(\bar{L}_{y_1}, \dots, \bar{L}_{y_P})$ in the resolved conifold. Moreover, the modulus y_i of the i -th brane in the resolved conifold is determined by the holonomy data (2.17)

$$y_i = \oint_{\partial D=\beta} \mathcal{A} + \int_D \mathcal{J} = g_s \left(R_i - i + P + \frac{1}{2} \right) \quad i = 1, \dots, P \quad (3.22)$$

We now proceed to verify this identification for the case when the Wilson loop operator is defined on the simplest knot, the unknot. When the deformed conifold geometry is defined by

$$z_1 z_4 - z_2 z_3 = \mu, \quad (3.23)$$

the unknot is parameterized by $(z_1, z_2, z_3, z_4) = (0, \sqrt{\mu}e^{i\theta}, -\sqrt{\mu}e^{-i\theta}, 0)$ with $0 \leq \theta \leq 2\pi$.

For the case of the unknot, the Wilson loop operator W_R in (2.3) is described by the configuration of D-branes in Figure 2¹⁹. The corresponding Lagrangian submanifolds end on the inner edge, thus accounting for the group theory bound $R_1^T \leq N$. This is consistent with the requirement that β should be non-contractible.

It was shown in [27], as reviewed in Appendix B, that the Wilson loop vev for the unknot can be rewritten as

$$\langle W_R \rangle = M(q) e^{-\sum_{n=1}^{\infty} \frac{e^{-nt}}{n[n]^2}} \left(\prod_{i<j} (1 - e^{-(x_i-x_j)}) \right) \prod_{i=1}^M \exp \sum_{n=1}^{\infty} \frac{e^{-nx_i} + e^{-n(t-x_i)}}{n[n]}, \quad (3.24)$$

up to unimportant factors we suppress here. Here $M(q) = \prod_{j=1}^{\infty} (1 - q^j)^{-j}$ is the MacMahon function, $t = g_s(N + M)$ and $x_i = g_s(R_i^T - i + M + \frac{1}{2})$, $i = 1, \dots, M$. This is exactly the A-model amplitude for the brane configuration in Figure 2²⁰, thus confirming our identification

$$\langle W_R \rangle = \langle (L_{x_1}, \dots, L_{x_M}) \rangle. \quad (3.25)$$

We also show in Appendix B that the Wilson loop vev can also be written as

$$\langle W_R \rangle = M(q) e^{-\sum_{n=1}^{\infty} \frac{e^{-nt}}{n[n]^2}} \left(\prod_{i<j} (1 - e^{-(y_i-y_j)}) \right) \prod_{i=1}^P \exp \sum_{n=1}^{\infty} \frac{e^{-ny_i} - e^{-n(t+y_i)}}{n[n]}, \quad (3.26)$$

¹⁹ Let us parameterize the resolved conifold by $|\lambda_1|^2 + \lambda_2|^2 - |\zeta_1|^2 - |\zeta_2|^2 = \text{Re } t$ up to $U(1)$ equivalence with charges $(1, 1, -1, -1)$. In Figures 2 and 3, the left, right, top, and bottom regions correspond to $|\lambda_1|^2 = 0, |\lambda_2|^2 = 0, |\zeta_1|^2 = 0$, and $|\zeta_2|^2 = 0$, respectively. L is given by $|\lambda_1|^2 - \text{Re } x = |\lambda_2|^2 - \text{Re } (t - x) = |\zeta_1|^2 = |\zeta_2|^2$, $\arg(\zeta_1 \zeta_2 \lambda_1 \lambda_2) = \pi$. When the conifold is singular the z and (λ, ζ) coordinates are related as $\begin{pmatrix} z_1 & z_2 \\ z_3 & z_4 \end{pmatrix} = \begin{pmatrix} \zeta_1 \\ \zeta_2 \end{pmatrix} \begin{pmatrix} -\lambda_2 & \lambda_1 \end{pmatrix}$.

²⁰The factor $\prod_{i<j} (1 - e^{-(x_i-x_j)})$ is the contribution from annulus diagrams between branes. This is essentially the Vandermonde determinant, i.e. the Weyl denominator. It demonstrates that the branes are fermions, as shown first in the mirror B-model [34]. The rest of (3.24), up to $M(q)$, can be computed by the topological vertex technology [34].

with $y_i = g_s(R_i - i + P + \frac{1}{2})$, $i = 1, \dots, P$, $t = g_s(N - P)$. This is exactly the A-model amplitude for the brane configuration in Figure 3, thus confirming our identification²¹

$$\langle W_R \rangle = \langle (\bar{L}_{y_1}, \dots, \bar{L}_{y_P}) \rangle. \quad (3.27)$$

In summary we have identified the bulk description of Wilson loop operators in Chern-Simons theory in terms of D-branes and anti-branes in the resolved conifold. Moreover, this identification has been explicitly verified for the case of the unknot.

4 Wilson loops as bubbling Calabi-Yau's

A geometric transition is a phenomenon in which a stack of D-branes is replaced by a new geometry with “flux”. More precisely, when the number of branes in the stack is large, the system is better described by a certain geometry where the appropriate fields that encode the charges of the branes are turned on. In physical string theory these fields are RR fluxes originally sourced by the D-branes. In topological string theory, the role of the fluxes is played by bulk gauge fields, namely the Kähler form and the B-field. The change in the geometry is such that the non-trivial cycle, which originally surrounds²² the branes and is homologically trivial, becomes a non-trivial cycle that supports the “flux”. There are by now many examples of this phenomenon. Here we will find a new class of geometric transitions in topological string theory.

It has been argued in [3, 6] that the D-branes realizing the half BPS straight Wilson lines in $\mathcal{N} = 4$ SYM can undergo transition to certain *bubbling* geometries that asymptote to $AdS_5 \times S^5$. To obtain these geometries one makes an ansatz for supergravity fields based on the knowledge of the symmetry of the branes describing the Wilson loops. One then imposes the BPS condition and finds that the supergravity solution is determined by simple data, namely a black-and-white pattern on a line as in Figure 4(a). It is expected that the data corresponds to the representation of the Wilson loop [3].

We found in section 3 that Wilson loop operators in Chern-Simons theory can be realized by a configuration of branes or anti-branes in the resolved conifold. When the

²¹ The same amplitude would arise if the branes ended on any of the four outer edges. One can convince oneself that they end on the lower-left edge by the following argument. In the convention of footnote 19, one can show that α is the trivial cycle in L if L ends on the lower-left or upper-right edge. β is trivial if L ends on the lower-right or upper-left edge. Since we have non-trivial holonomy of a flat connection along β , β has to be non-trivial, and thus L has to end on either the lower-left or upper-right edge. By carefully keeping track of the orientation of the cycle β , one can show that increasing the holonomy is gauge equivalent to moving the branes toward the lower-left. Since one can increase the holonomy without bound, the branes must end on the lower-left edge. Such L is given by the equations $|\lambda_1|^2 = |\lambda_2|^2 - \text{Re}(t + y) = |\zeta_1|^2 - \text{Re} y = |\zeta_2|^2$, $\arg(\zeta_1 \zeta_2 \lambda_1 \lambda_2) = \pi$.

²² Let W be the world-volume of the brane, and M a homologically trivial cycle. We say that M surrounds W if there is a chain N such that $\partial N = M$ and if the intersection number of N and W is non-zero.

number of D-branes in a stack is large we expect that the system has a better description in terms of pure geometry. The D-branes wrap a Lagrangian submanifold L of topology $\mathbb{R}^2 \times \mathbb{S}^1$. The neighborhood of the submanifold, modeled by the normal bundle, is locally $\mathbb{R}^5 \times \mathbb{S}^1$. A contractible \mathbb{S}^2 in the transverse \mathbb{R}^3 surrounds the branes. The geometric transition of the D-branes makes the \mathbb{S}^2 non-trivial while making the \mathbb{S}^1 contractible. More precisely, the topology change is described by a surgery procedure: we cut out a tubular neighborhood of topology $(3\text{-ball}) \times \mathbb{R}^2 \times \mathbb{S}^1$ from the ambient space X and glue in a region of topology $\mathbb{S}^2 \times \mathbb{R}^2 \times (\text{disk})$ to get a new space X' . A relative 2-cycle with boundary on L combines with the disk to become a 2-cycle in X' .

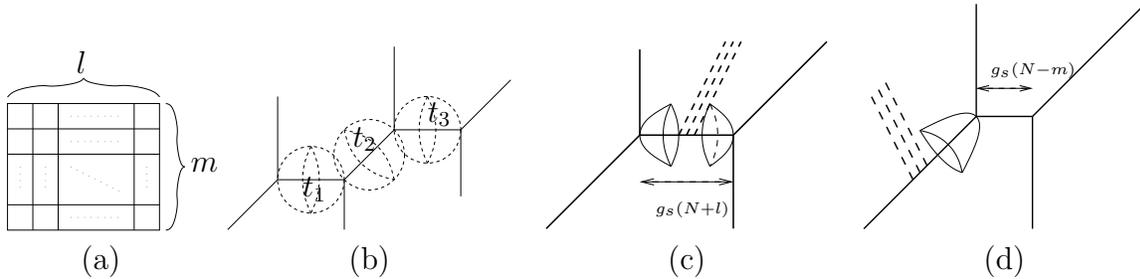


Figure 5: The simplest example of the correspondence between a Wilson loop and a bubbling geometry. The Wilson loop along the unknot in the $U(N)$ representation specified by the Young tableau (a) is equivalent to the toric Calabi-Yau manifold given by the web diagram (b). The Kähler moduli in (b) are given by $t_1 = g_s m$, $t_2 = g_s l$, $t_3 = g_s(N - m)$. The bubbling CY manifold (b) arises from geometric transition of l branes in (c) as well as m anti-branes in (d).

Let us now specialize to the Wilson loop along the unknot, in a representation of the form Figure 5(a). The Wilson loop is realized by a stack of l Lagrangian D-branes on the inner edge at positions $x_i = g_s(l + m - i + 1/2)$, $i = 1, \dots, l$. These branes live in the resolved conifold with Kähler modulus $t = g_s(N + l)$. We propose that when l and m are large, these branes undergo geometric transition to the toric Calabi-Yau manifold whose toric web diagram is shown in 5(b). The three Kähler moduli are $t_1 = g_s m$, $t_2 = g_s l$, $t_3 = g_s(N - m)$. Note that the new geometry has topology that is precisely as described above. The contractible sphere that originally surrounded the branes become a non-trivial cycle of size $g_s l$. The two holomorphic disks that originally ended on the branes become spheres of sizes $g_s m$ and $g_s(N - m)$. Our proposal is supported by the explicit computation for the unknot. If we substitute $x_i = g_s(l + m - i + 1/2)$ into the open+closed string partition function (3.24) in the brane set up of Figure 5(c), it

becomes²³

$$M(q)^2 \exp \sum_{n=1}^{\infty} \frac{1}{n[n]^2} \left(-e^{-nt_1} - e^{-nt_2} - e^{-nt_3} + e^{-n(t_1+t_2)} + e^{-n(t_2+t_3)} - e^{-n(t_1+t_2+t_3)} \right) \quad (4.28)$$

This is precisely the closed string amplitude for the bubbling Calabi-Yau in Figure 5(b), computed using mirror symmetry and integrality²⁴! This constitutes very strong evidence for our proposal for the geometric transition.

In section 3 we showed that the same Wilson loop is realized by a stack of m anti-branes on an outer edge with holonomies $y_i = g_s(l + m - i + 1/2)$, $i = 1, \dots, m$ turned on. (See Figure 5(d).) The anti-branes live in the resolved conifold with $t = g_s(N - m)$. These anti-branes also undergo geometric transition. The resulting geometry is the same as for the branes on the inner edge. In this case the 2-sphere surrounding the anti-branes acquires size $g_s m$, and one 2-sphere of size $g_s l$ arises from a holomorphic disk ending on the anti-branes. The open+closed string partition function (3.26) for the anti-branes again becomes²⁵ the closed string partition function (4.28) after substituting the values for y_i .

Let us now discuss the Wilson loop along the unknot in the general representation R . It is convenient to parameterize R in terms of lengths l_i of the edges as in Figure 4(a). The open+closed string partition functions (3.24) and (3.26) both become, after substituting the values for holonomies,

$$M(q)^{m+1} \exp \sum_{n=1}^{\infty} \frac{1}{n[n]^2} \left(- \sum_{1 \leq i \leq 2m+1} e^{-nt_i} + \sum_{1 \leq i \leq 2m} e^{-n(t_i+t_{i+1})} - \sum_{1 \leq i \leq 2m-1} e^{-n(t_i+t_{i+1}+t_{i+2})} \dots - e^{-n(t_1+\dots+t_{2m+1})} \right) \quad (4.29)$$

We recognize this as the closed string partition function for the toric Calabi-Yau whose toric diagram is shown in Figure 4(b) [34]! This complicated geometry arises via geometric transition of branes or anti-branes. The description in terms of geometry is more appropriate when l_i , hence the cycles, are large. These Calabi-Yau manifolds provide a novel representation of knot invariants in Chern-Simons theory.

In the forthcoming paper [29] we will show that the open GV invariants for an arbitrary knot determine the closed GV invariants of the bubbling CY geometry as well as discuss generalization of the newly found class of geometric transitions.

²³For precise agreement we should include $\xi(q)^l$ in (3.24) where $\xi(q) = \prod_{j=1}^{\infty} (1 - q^j)^{-1}$. This factor does not contribute to perturbative amplitudes because of its modular property [28].

²⁴See subsection 9.1 of [34]

²⁵ Insert $\xi(q)^m$ to (3.26) for precise agreement.

Acknowledgments

We thank Vincent Bouchard, Laurent Freidel, Amihay Hanany, Amir-Kian Kashani-Poor, Hiroshi Ooguri, and Johannes Walcher for discussion. We thank the Aspen Center for Physics where this project was initiated. The research of T.O. is supported in part by the NSF grants PHY-9907949 and PHY-0456556. Research of J.G. is supported in part by funds from NSERC of Canada and by MEDT of Ontario.

Appendix

A Wilson loops as world-sheet instantons

As in AdS/CFT, Wilson loops in Chern-Simons theory are expected to be realized by non-compact world-sheets [16, 35] in the resolved conifold. In this appendix we explain how this works and point out that the description in terms of world-sheets naturally gives rise to the generating functional of Wilson loops originally obtained in [20]. The generating functional is the amplitude for branes wrapping a certain Lagrangian submanifold. Conversely, this implies that exact computation of the brane amplitude amounts to exact quantization of string theory around a classical string solution.

In Chern-Simons perturbation theory, the expectation value of the Wilson loop operator in the fundamental representation is computed by summing Feynman diagrams with external legs ending on the loop:

$$\langle W_{\square} \rangle = \langle \text{Tr} P e^{\oint A} \rangle = \text{Diagram 1} + \text{Diagram 2} + \text{Diagram 3} + \text{Diagram 4} + \text{Diagram 5} + \dots \quad (\text{A.30})$$

Here the filled circles are the end points of the gauge field propagators, and are integrated along the Wilson loop. When the Feynman diagrams are drawn as fat graphs, they can directly be viewed as infinitely thin open string world-sheets [19]. To provide for a string theory description, we place an extra holomorphic world-sheet that has the loop as its boundary because the boundary of the world-sheet is the Wilson loop. This surface is unique and is given as follows. The equation for the deformed conifold is given in (3.23). Let us introduce w coordinates by $z_1 = w_1 + iw_2$, $z_4 = w_1 - iw_2$, $z_2 = w_3 + iw_4$, $z_3 = -w_3 + iw_4$. Then the equation becomes

$$w_1^2 + w_2^2 + w_3^2 + w_4^2 = \mu, \quad w_i \in \mathbf{C}, \quad i = 1, 2, 3, 4. \quad (\text{A.31})$$

Let us write $w_i = a_i + ib_i$ with real a_i, b_i . The S^3 is the real locus ($b_i = 0$) of the hypersurface. A knot can be parameterized as

$$a_i = f_i(\theta), \quad 0 \leq \theta \leq 2\pi, \quad (\text{A.32})$$

where $f_i(\theta)$ are real functions satisfying $\sum_i f_i(\theta)^2 = \mu$. Then the holomorphic surface is given by

$$w_i(\zeta) = f_i(\zeta), \quad \zeta \in \mathbf{C}, \quad \zeta \sim \zeta + 2\pi, \quad \text{Im} \zeta \geq 0. \quad (\text{A.33})$$

Thin open string world-sheets should then be glued to the boundary of the holomorphic surface. In other words, we are quantizing the open string theory around a classical string solution represented by the holomorphic world-sheet. As in AdS/CFT we need to cut off the infinite area of the surface. After IR regularization the contribution of the infinite holomorphic surface is simply $e^{-\text{Area}}$. By subtracting the area, string theory around the holomorphic world-sheet computes the Wilson loop vev.

It is easy to generalize this consideration to an arbitrary multi-trace case

$$\langle W_{\vec{k}} \rangle := \left\langle \prod_{j=1}^{\infty} \left(\text{Tr} P e^{j \oint A} \right)^{k_j} \right\rangle. \quad (\text{A.34})$$

\vec{k} is an infinite vector of non-negative integers. If we know these expectation values we can compute the vev of the Wilson loop in an arbitrary representation with the help of the Frobenius relation. The computation of such an operator is done by expanding the string theory around a classical string solution in which we place k_1 singly wrapped surfaces, k_2 doubly wrapped surfaces, etc. The classical configuration involves a total of $\sum k_j$ distinct world-sheets. Note that there are quantum fluctuations that connect them. They represent the interactions among fundamental strings.

The IR regularization of the world-sheet can be conveniently done by introducing M non-compact D-branes on which the second boundary of the large world-sheet ends.

These D-branes wrap a Lagrangian L . It is in fact convenient to deal at once with configurations with all possible \vec{k} (with $k_j = 0$ for all $j > M$). Let s be the area of the holomorphic surface. The idea is that the surface appears in the perturbative quantization of topological strings in the background with non-compact D-branes. Let us denote by V the $M \times M$ holonomy matrix for the gauge field on L along the boundary of the surface. Because the world-volume is non-compact, the gauge field on the non-compact branes is essentially non-dynamical. The contribution from the stack of world-sheet instantons specified by \vec{k} picks up the factors $\prod_{j=1}^{\infty} (\text{Tr} V^j)^{k_j}$ from the holonomy on the second boundary. The open string partition function $Z(V)$ of the system with branes is given by

$$Z(V) = \sum_{\vec{k}} \frac{1}{z_{\vec{k}}} \langle W_{\vec{k}} \rangle \prod_{j=1}^{\infty} (\text{Tr}(e^{-s} V)^j)^{k_j}. \quad (\text{A.35})$$

$1/z_{\vec{k}} = 1/\prod_j (k_j!) j^{k_j}$ is the symmetry factor. Up to e^{-s} this agrees with the generating functional of Wilson loops obtained in [20] through consideration in the open string channel. Here we provided a closed string channel derivation.

Let us now follow the conifold transition to the resolved side. The Gopakumar-Vafa duality implies that $Z(V)$ can be identified with the partition function of topological strings in the resolved conifold, in the presence of non-compact branes with holonomy V . The contribution to the coefficient of $\prod_{j=1}^{\infty} (\text{Tr}(e^{-s}V)^j)^{k_j}$ now comes from a stack of world-sheet instantons. Their boundaries are on L and they are wrapped multiply in the way specified by \vec{k} . The branes provide IR regularization. Thus our conclusion is that the Wilson loop $\prod_{j=1}^{\infty} (\text{Tr}P e^{\oint A})^{k_j}$ is identified with the stack of non-compact world-sheet instantons whose wrapping numbers are $\vec{k} = (k_1, k_2, \dots)$. The exact computation of the brane amplitude (A.35), which is possible for unknot, then leads to exact quantization of string theory around the classical string solution. Note that the interactions between world-sheets, corresponding to quantum fluctuations that connect world-sheets, arise in the perturbative computation of the brane amplitude.

B Wilson loops as crystals

In this section we revisit the crystal description of the Wilson loop vev for the unknot, developed in [27]. Besides being interesting on its own right, our aim here is to use such crystals to facilitate the computations showing that the Wilson loop vev equals the A-model amplitudes of branes, anti-branes, and the bubbling Calabi-Yau's²⁶.

Let R be the representation corresponding to a Young diagram. Consider the three dimensional region shown in Figure 6. A unit cube in the region is considered to be an atom. Outside the region is the air. We regard the region as the initial crystal configuration, which is specified by Young diagram R in Figure 4(a). An atom can melt away only if three of its faces are already exposed to the air [26]. Now let us consider the ensemble of all crystal configurations in which some atoms have melted away. The partition function is defined by summing over all melted crystal configurations with Boltzman weight q^E , where $E = (\text{number of removed boxes})$. It was shown in [27] that the unnormalized expectation value of the Wilson loop $\langle W_R \rangle$ for unknot agrees with the crystal partition function up to some factors²⁷.

This type of crystal melting problem can be treated efficiently using the free CFT techniques [26]. For our purposes, all the reader needs to know is the commutation relation of two operators $\Gamma_{\pm}(z)$ and how they act on the vacuum²⁸:

$$\Gamma_+(z_+) \Gamma_-(z_-) = \frac{1}{1 - z_+/z_-} \Gamma_-(z_-) \Gamma_+(z_+), \quad \Gamma_+(z)|0\rangle = \langle 0|\Gamma_-(z) = 0. \quad (\text{B.36})$$

²⁶The computations can in principle be performed starting with the expression $\langle W_R \rangle \sim \det_{1 \leq i, j \leq N} (q^{j(R_i - i)})$, though the crystals provide more transparent methods.

²⁷ For the prefactors that play no role for us, see [27].

²⁸ If the reader wishes to understand how the crystal melting problem is translated to the free CFT expressions, formulas like $\Gamma_+(1)|R\rangle = \sum_{R \prec Q} |Q\rangle$ that can be found in [26].

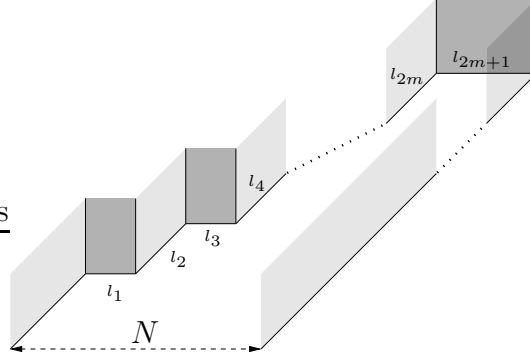


Figure 6: Crystal configuration before melting. This crystal corresponds to Figure 4.

The partition function $\langle W_R \rangle$ can be expressed in several different ways. Here we consider the expressions which differ only²⁹ in the way the Young diagram R is parametrized. The first parametrization uses the number R_i of boxes in the i -th row. The second uses the number R_i^T of boxes in the i -th column. The third uses the length l_i of i -th edge. See Figures 1 and 4(a) for examples.

In the parametrization in terms of the number R_i of boxes in the i -th row, the Wilson loop vev is given by

$$\begin{aligned}
 \langle W_R \rangle = & \langle 0 | \left[\prod_{i=R_1}^{\infty} \Gamma_+(q^i) \right] \Gamma_-(q^{R_1-1}) \left[\prod_{i=R_2-1}^{R_1-2} \Gamma_+(q^i) \right] \Gamma_-(q^{R_2-2}) \dots \\
 & \times \Gamma_-(q^{R_P-P}) \left[\prod_{i=-P}^{R_P-P-1} \Gamma_+(q^i) \right] \left[\prod_{i=-N}^{-P-1} \Gamma_-(q^i) \right] | 0 \rangle. \quad (\text{B.37})
 \end{aligned}$$

(B.36) allows one to compute this and obtain (3.26) that is the partition function in the presence of anti-branes on the outer edge. The special case $P = 1$ of this interpretation was found in [36].

The parametrization in terms of R_i^T , the number of boxes in each column, naturally relates the crystal to the branes in section 3. This is the parametrization considered in

²⁹ Our considerations here are all in the closed string slicing as defined in [27]. There is also the open string slicing that is useful for relating $\langle W_R \rangle$ to the Wilson loop vev.

[27]. It was found that³⁰

$$\begin{aligned}
\langle W_R \rangle &= \langle 0 | \left[\prod_{i=1}^{\infty} \Gamma_+(q^{i-1}) \right] \left[\prod_{i=1}^{R_M^T} \Gamma_-(q^{-i}) \right] \Gamma_+(q^{-(R_M^T+1)}) \left[\prod_{i=R_M^T+2}^{R_{M-1}^T+1} \Gamma_-(q^{-i}) \right] \dots \\
&\times \left[\prod_{i=R_2^T+M}^{R_1^T+M-1} \Gamma_-(q^{-i}) \right] \Gamma_+(q^{-(R_1^T+M)}) \left[\prod_{i=R_1^T+M+1}^{N+M} \Gamma_-(q^{-i}) \right] |0\rangle. \quad (\text{B.38})
\end{aligned}$$

One can derive (3.24) from this.

The parametrization in terms of l_i is useful for relating the crystal to the bubbling geometry. $\langle W_R \rangle$ is written as

$$\begin{aligned}
\langle W_R \rangle &= \langle 0 | \left[\prod_{i=1}^{\infty} \Gamma_+(q^{i-1}) \right] \left[\prod_{i=1}^{l_1} \Gamma_-(q^{-i}) \right] \left[\prod_{i=1}^{l_2} \Gamma_+(q^{-l_1-i}) \right] \dots \\
&\times \left[\prod_{i=1}^{l_{2m-1}} \Gamma_-(q^{-l_1-l_2-\dots-l_{2m-2}-i}) \right] \left[\prod_{i=1}^{l_{2m}} \Gamma_+(q^{-l_1-l_2-\dots-l_{2m-1}-i}) \right] \\
&\times \left[\prod_{i=1}^{l_{2m+1}} \Gamma_-(q^{-l_1-l_2-\dots-l_{2m-1}-l_{2m}-i}) \right] |0\rangle. \quad (\text{B.39})
\end{aligned}$$

Using (B.36), one can show that this reduces to (4.29). The crystal is directly related to the bubbling geometry as one sees by comparing Figures 4 and 6.

C Target space theory of open topological strings

Let us consider the case of a single A-brane wrapping a Lagrangian submanifold L of a Calabi-Yau manifold M . In A-model, only (the cohomology class of) the symplectic structure $\omega = \frac{1}{2}\omega_{\mu\nu}dx^\mu \wedge dx^\nu$ of M , not the whole Kähler structure, is relevant. When the B-field vanishes, the equation of motion for the gauge field is simply $F \equiv dA = 0$. When the B-field is turned on the equation of motion should be generalized so that it is invariant under the gauge transformation $B \rightarrow B + d\Lambda$, $A \rightarrow A - \Lambda$ ³¹. The minimal gauge invariant equation of motion is

$$F + B = 0. \quad (\text{C.40})$$

³⁰ The expressions in (B.37-B.39) differ in the parametrization of the Young diagram as well as the overall rescaling in the arguments of Γ_{\pm} . Neither affects the amplitude. The overall rescaling is equivalent to conjugating all the operators by a power of q^{L_0} , where L_0 is the Virasoro zero mode [26].

³¹The notation for gauge fields in this appendix differs from the rest of the paper. Here A is a hermitian connection, and $\mathcal{A} = \phi - iA$ is its complexification.

For a single Lagrangian A-brane, one real modulus is given, when $B = 0$, by the holonomy $\oint A$ along a non-trivial 1-cycle of L . This is again to be promoted to a gauge-invariant combination. The minimal combination is

$$\oint_{\partial D} A + \int_D B, \quad (\text{C.41})$$

where $D \subset M$ is a disk (or more generally a surface with boundary) whose boundary is the 1-cycle³².

In topological field theory, all moduli are complex. There must be another real modulus associated with the 1-cycle that combines with (C.41) to form a complex modulus. The existence of the additional modulus can be understood as follows [37].

Let us consider an infinitesimal deformation of L that preserves the condition that the submanifold is Lagrangian. An infinitesimal deformation corresponds to a normal vector field v , i.e., a section of the normal bundle $TM|_L/TL$. We can think of v as a vector field defined in a neighborhood of L

$$v = v^\mu \partial_\mu \quad (\text{C.42})$$

(indices are for M coordinates), up to a vector field ξ , defined in the same domain, such that $\xi|_L \in TL$. ω is preserved by the deformation if and only if

$$L_v \omega = 0 \quad (\text{C.43})$$

where L_v is the Lie derivative. By contracting v with the symplectic form ω , one can form a 1-form in the neighborhood of L :

$$i_v \omega = \omega_{\mu\nu} v^\mu dx^\nu. \quad (\text{C.44})$$

$i_v \omega$ is closed and its restriction $i_v \omega|_L$ defines a cohomology class of L . $i_v \omega|_L$ is exact if and only if v is a Hamiltonian vector field: $v = (\omega^{-1})^{\mu\nu} \partial_\nu f$ for some function f . Indeed it is known that two Lagrangian submanifolds related by a Hamiltonian deformation defines the same open string theory [37]. Infinitesimally, the deformation modulus is given by $\oint_{\partial D} i_v \omega$.

The modulus for a finite deformation is known to be given (for a single brane) by the symplectic area of the disk³³

$$\int_D \omega. \quad (\text{C.45})$$

³² Since $b_1(M) = 0$, the 1-cycle of L has to be the boundary of some chain D in M .

³³ When D is a holomorphically embedded disk, the symplectic area agrees with the area with respect to the Kähler metric of M .

One can easily check that the variation of (C.45) is proportional to $\oint_{\partial D} i_v \omega$.

The description of the deformation modulus in the above two paragraphs is rather unsatisfactory because unlike (C.41), (C.45) does not depend on a field of the world-volume theory. We now point out that the correct description of the brane, namely the Chern-Simons theory with a complex gauge group, generalizes (C.45) into a form that is in parallel with (C.41).

In string theory, all deformations of the theory must appear in the physical spectrum. As Witten showed in [19], the spectrum comes solely from $H^1(L)$. For N coincident branes, this gives rise to $U(N)$ theory when a reality condition is imposed on the string field. To account for deformations of the Lagrangian submanifold, however, it is more natural not to impose the reality condition [37]. Thus the gauge field is a complex field, and the gauge group is $GL(N, \mathbb{C})$. We write $A + i\phi$ for the complex gauge field.

To understand the meaning of the imaginary part of the gauge field, let us consider the vertex operators for the gauge fields. Let us use coordinates X^a to parameterize L , and Y^a for transverse directions so that $X^a + iY^a$ are complex coordinates of M . Topological string theory is a version of bosonic string theory [19]. The “fixed” vertex operators [38] for the real gauge fields A_a are the fermions χ^a in the notation of [19]. The corresponding “integrated” vertex operators are $\{b_0, \chi^a\}$, which turn out to be $\partial_\tau X^a$. (τ is the parameter for the boundary of a world-sheet, and $X^a(z = \sigma + i\tau)$ are the embedding coordinates.) Thus the “integrated” vertex operators for the imaginary gauge fields ϕ_a are $i\partial_t X^a$. In topological A-model, only the field configurations such that $X^a + iY^a$ is holomorphic in z contribute. For such configurations $i\partial_\tau X^a = -i\partial_\sigma Y^a$. It is well-known that integrating these vertex operators induces transverse deformations of the brane. Thus we have shown that the imaginary gauge fields give rise to deformations of the brane.

Our conclusion, which is in agreement with some of the literature [37], is that in topological A-model the natural gauge group for the Chern-Simons theory on A-branes is a complex gauge group. This obviously raises the issue of non-perturbative definition because the path-integral seems to be divergent. Our attitude here is that only the perturbative definition of the Chern-Simons theory is relevant. This is consistent with the fact that topological string theory is defined only perturbatively.

Once we accept the complex gauge group, there is natural generalization of (C.45) for the real modulus:

$$\oint_{\partial D} \phi + \int_D \omega \tag{C.46}$$

In other words, the complex modulus corresponding to the 1-cycle is

$$\oint_{\partial D} \mathcal{A} + \int_D \mathcal{J}, \tag{C.47}$$

where $\mathcal{A} \equiv \phi - iA$, $\mathcal{J} \equiv (\omega - iB)$. Note that this expression is invariant under the

complex generalization of the B-field gauge transformation

$$B + i\omega \rightarrow B + i\omega + d(\Lambda + i\lambda), \quad A + i\phi \rightarrow A + i\phi - (\Lambda + i\lambda). \quad (\text{C.48})$$

The minimal non-Abelian gauge invariant equation of motion for the open strings interacting with closed strings is

$$\mathcal{F} + \mathcal{J}1_{N \times N} = 0, \quad (\text{C.49})$$

where $\mathcal{F} = d\mathcal{A} + \mathcal{A}^2$.

For a promising approach to the target space theory, see [39].

References

- [1] J. Gomis and F. Passerini, “Holographic Wilson loops,” [hep-th/0604007](#).
- [2] N. Drukker and B. Fiol, “All-genus calculation of Wilson loops using D-branes,” *JHEP* **02** (2005) 010, [hep-th/0501109](#).
- [3] S. Yamaguchi, “Bubbling geometries for half BPS Wilson lines,” [hep-th/0601089](#).
- [4] S.-J. Rey and J.-T. Yee, “Macroscopic strings as heavy quarks in large N gauge theory and anti-de Sitter supergravity,” *Eur. Phys. J.* **C22** (2001) 379–394, [hep-th/9803001](#).
- [5] J. M. Maldacena, “Wilson loops in large N field theories,” *Phys. Rev. Lett.* **80** (1998) 4859–4862, [hep-th/9803002](#).
- [6] O. Lunin, “On gravitational description of Wilson lines,” *JHEP* **06** (2006) 026, [hep-th/0604133](#).
- [7] J. Gomis and C. Romelsberger, “Bubbling defect CFT’s,” *JHEP* **08** (2006) 050, [hep-th/0604155](#).
- [8] H. Lin, O. Lunin, and J. M. Maldacena, “Bubbling AdS space and 1/2 BPS geometries,” *JHEP* **10** (2004) 025, [hep-th/0409174](#).
- [9] S. Yamaguchi, “Wilson loops of anti-symmetric representation and D5- branes,” *JHEP* **05** (2006) 037, [hep-th/0603208](#).
- [10] S. A. Hartnoll and S. Prem Kumar, “Multiply wound Polyakov loops at strong coupling,” *Phys. Rev.* **D74** (2006) 026001, [hep-th/0603190](#).

- [11] K. Okuyama and G. W. Semenoff, “Wilson loops in $N = 4$ SYM and fermion droplets,” *JHEP* **06** (2006) 057, [hep-th/0604209](#).
- [12] S. A. Hartnoll and S. P. Kumar, “Higher rank Wilson loops from a matrix model,” *JHEP* **08** (2006) 026, [hep-th/0605027](#).
- [13] S. Giombi, R. Ricci, and D. Trancanelli, “Operator product expansion of higher rank Wilson loops from D-branes and matrix models,” *JHEP* **10** (2006) 045, [hep-th/0608077](#).
- [14] T.-S. Tai and S. Yamaguchi, “Correlator of fundamental and anti-symmetric Wilson loops in AdS/CFT correspondence,” [hep-th/0610275](#).
- [15] J. Gomis and F. Passerini, “Wilson loops as D3-branes,” [hep-th/0612022](#).
- [16] R. Gopakumar and C. Vafa, “On the gauge theory/geometry correspondence,” *Adv. Theor. Math. Phys.* **3** (1999) 1415–1443, [hep-th/9811131](#).
- [17] A. Neitzke and C. Vafa, “Topological strings and their physical applications,” [hep-th/0410178](#).
- [18] M. Marino, “Chern-Simons theory, matrix models, and topological strings,” Oxford, UK: Clarendon (2005) 197 p.
- [19] E. Witten, “Chern-Simons gauge theory as a string theory,” *Prog. Math.* **133** (1995) 637–678, [hep-th/9207094](#).
- [20] H. Ooguri and C. Vafa, “Knot invariants and topological strings,” *Nucl. Phys.* **B577** (2000) 419–438, [hep-th/9912123](#).
- [21] J. M. F. Labastida and M. Marino, “Polynomial invariants for torus knots and topological strings,” *Commun. Math. Phys.* **217** (2001) 423–449, [hep-th/0004196](#).
- [22] J. M. F. Labastida, M. Marino, and C. Vafa, “Knots, links and branes at large N ,” *JHEP* **11** (2000) 007, [hep-th/0010102](#).
- [23] M. Marino and C. Vafa, “Framed knots at large N ,” [hep-th/0108064](#).
- [24] C. H. Taubes, “Lagrangians for the Gopakumar-Vafa conjecture,” *Adv. Theor. Math. Phys.* **5** (2001) 139–163, [math.dg/0201219](#).
- [25] S. Koshkin, “Conormal bundles to knots and the Gopakumar-Vafa conjecture,” [math.DG/0503248](#).
- [26] A. Okounkov, N. Reshetikhin, and C. Vafa, “Quantum Calabi-Yau and classical crystals,” [hep-th/0309208](#).

- [27] T. Okuda, “Derivation of Calabi-Yau crystals from Chern-Simons gauge theory,” *JHEP* **03** (2005) 047, [hep-th/0409270](#).
- [28] N. Saulina and C. Vafa, “D-branes as defects in the Calabi-Yau crystal,” [hep-th/0404246](#).
- [29] J. Gomis and T. Okuda. To appear.
- [30] C. Vafa, “Brane/anti-brane systems and $U(N|M)$ supergroup,” [hep-th/0101218](#).
- [31] T. Okuda and T. Takayanagi, “Ghost D-branes,” *JHEP* **03** (2006) 062, [hep-th/0601024](#).
- [32] S. Elitzur, G. W. Moore, A. Schwimmer, and N. Seiberg, “Remarks on the canonical quantization of the Chern-Simons- Witten theory,” *Nucl. Phys.* **B326** (1989) 108.
- [33] E. Witten, “Quantum field theory and the Jones polynomial,” *Commun. Math. Phys.* **121** (1989) 351.
- [34] M. Aganagic, A. Klemm, M. Marino, and C. Vafa, “The topological vertex,” *Commun. Math. Phys.* **254** (2005) 425–478, [hep-th/0305132](#).
- [35] A. Dymarsky, S. Gubser, Z. Guralnik, and J. M. Maldacena, “Calibrated surfaces and supersymmetric Wilson loops,” [hep-th/0604058](#).
- [36] N. Halmagyi, A. Sinkovics, and P. Sulkowski, “Knot invariants and Calabi-Yau crystals,” *JHEP* **01** (2006) 040, [hep-th/0506230](#).
- [37] P. S. Aspinwall, “D-branes on Calabi-Yau manifolds,” [hep-th/0403166](#).
- [38] J. Polchinski, “String theory. Vol. 1: An introduction to the bosonic string,” Cambridge, UK: Univ. Pr. (1998) 402 p.
- [39] R. P. Thomas, “Moment maps, monodromy and mirror manifolds,” [math.dg/0104196](#).